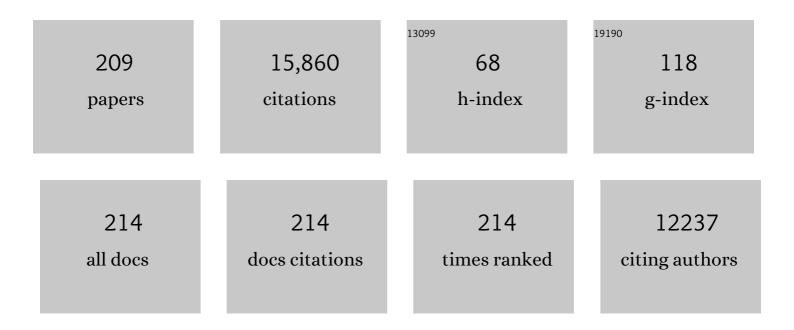
## Chun Hu

List of Publications by Year in descending order

Source: https://exaly.com/author-pdf/6653506/publications.pdf Version: 2024-02-01



| #  | Article   | IF   | CITATIONS |
|----|---|------|-----------|
| 1  | Effective Photocatalytic Disinfection of <i>E. coli</i> K-12 Using<br>AgBrâ^Agâ^Bi <sub>2</sub> WO <sub>6</sub> Nanojunction System Irradiated by Visible Light: The Role of<br>Diffusing Hydroxyl Radicals. Environmental Science & Technology, 2010, 44, 1392-1398. | 10.0 | 557       |
| 2  | Ag/AgBr/TiO2Visible Light Photocatalyst for Destruction of Azodyes and Bacteria. Journal of Physical Chemistry B, 2006, 110, 4066-4072.   | 2.6  | 552       |
| 3  | Plasmon-Induced Photodegradation of Toxic Pollutants with Agâ^'AgI/Al <sub>2</sub> O <sub>3</sub><br>under Visible-Light Irradiation. Journal of the American Chemical Society, 2010, 132, 857-862.   | 13.7 | 541       |
| 4  | Electronic Structure Modulation of Graphitic Carbon Nitride by Oxygen Doping for Enhanced<br>Catalytic Degradation of Organic Pollutants through Peroxymonosulfate Activation. Environmental<br>Science & Technology, 2018, 52, 14371-14380.                          | 10.0 | 455       |
| 5  | New Insights into the Generation of Singlet Oxygen in the Metal-Free Peroxymonosulfate Activation<br>Process: Important Role of Electron-Deficient Carbon Atoms. Environmental Science &<br>Technology, 2020, 54, 1232-1241.  | 10.0 | 400       |
| 6  | Degradation of Acid Orange 7 using magnetic AgBr under visible light: The roles of oxidizing species.<br>Chemosphere, 2009, 76, 1185-1191.  | 8.2  | 386       |
| 7  | Removal of phosphate by mesoporous ZrO2. Journal of Hazardous Materials, 2008, 151, 616-622.  | 12.4 | 326       |
| 8  | AgBr-Ag-Bi2WO6 nanojunction system: A novel and efficient photocatalyst with double visible-light active components. Applied Catalysis A: General, 2009, 363, 221-229.  | 4.3  | 304       |
| 9  | Enhanced photodegradation of toxic organic pollutants using dual-oxygen-doped porous g-C3N4:<br>Mechanism exploration from both experimental and DFT studies. Applied Catalysis B: Environmental,<br>2019, 248, 1-10.   | 20.2 | 291       |
| 10 | Degradation of selected pharmaceuticals in aqueous solution with UV and UV/H2O2. Water Research, 2009, 43, 1766-1774.   | 11.3 | 288       |
| 11 | Mechanism of Catalytic Ozonation in<br>Fe <sub>2</sub> O <sub>3</sub> /Al <sub>2</sub> O <sub>3</sub> @SBA-15 Aqueous Suspension for<br>Destruction of Ibuprofen. Environmental Science & Technology, 2015, 49, 1690-1697.  | 10.0 | 286       |
| 12 | Photodegradation of tetracycline and formation of reactive oxygen species in aqueous tetracycline solution under simulated sunlight irradiation. Journal of Photochemistry and Photobiology A: Chemistry, 2008, 197, 81-87.   | 3.9  | 249       |
| 13 | Enhanced Fenton Catalytic Efficiency of γ-Cu–Al <sub>2</sub> O <sub>3</sub> by<br>Ïf-Cu <sup>2+</sup> –Ligand Complexes from Aromatic Pollutant Degradation. Environmental Science<br>& Technology, 2015, 49, 8639-8647.  | 10.0 | 247       |
| 14 | Photodegradation and toxicity changes of antibiotics in UV and UV/H2O2 process. Journal of Hazardous Materials, 2011, 185, 1256-1263.   | 12.4 | 240       |
| 15 | Photocatalytic Degradation of Pathogenic Bacteria with Agl/TiO2under Visible Light Irradiation.<br>Langmuir, 2007, 23, 4982-4987.   | 3.5  | 217       |
| 16 | Surface oxygen vacancy inducing peroxymonosulfate activation through electron donation of pollutants over cobalt-zinc ferrite for water purification. Applied Catalysis B: Environmental, 2020, 270, 118874.  | 20.2 | 207       |
| 17 | Catalytic Ozonation of Selected Pharmaceuticals over Mesoporous Alumina-Supported Manganese<br>Oxide. Environmental Science & Technology, 2009, 43, 2525-2529.  | 10.0 | 203       |
| 18 | Efficient Destruction of Pollutants in Water by a Dual-Reaction-Center Fenton-like Process over<br>Carbon Nitride Compounds-Complexed Cu(II)-CuAlO <sub>2</sub> . Environmental Science &<br>Technology, 2018, 52, 4294-4304.   | 10.0 | 203       |

| #  | Article  | IF   | CITATIONS |
|----|--|------|-----------|
| 19 | Unraveling the High-Activity Origin of Single-Atom Iron Catalysts for Organic Pollutant Oxidation via Peroxymonosulfate Activation. Environmental Science & Technology, 2021, 55, 8318-8328.   | 10.0 | 198       |
| 20 | Indirect Photodegradation of Amine Drugs in Aqueous Solution under Simulated Sunlight.<br>Environmental Science & Technology, 2009, 43, 2760-2765.   | 10.0 | 195       |
| 21 | Effects of disinfectant and biofilm on the corrosion of cast iron pipes in a reclaimed water distribution system. Water Research, 2012, 46, 1070-1078.   | 11.3 | 193       |
| 22 | Plasmon-Assisted Degradation of Toxic Pollutants with Agâ^'AgBr/Al <sub>2</sub> O <sub>3</sub> under<br>Visible-Light Irradiation. Journal of Physical Chemistry C, 2010, 114, 2746-2750.  | 3.1  | 186       |
| 23 | Visible-Light-Induced Photocatalytic Degradation of Azodyes in Aqueous AgI/TiO2Dispersion.<br>Environmental Science & Technology, 2006, 40, 7903-7907.   | 10.0 | 180       |
| 24 | 4-Phenoxyphenol-Functionalized Reduced Graphene Oxide Nanosheets: A Metal-Free Fenton-Like<br>Catalyst for Pollutant Destruction. Environmental Science & Technology, 2018, 52, 747-756.   | 10.0 | 180       |
| 25 | Enhanced Fenton degradation of Rhodamine B over nanoscaled Cu-doped LaTiO3 perovskite. Applied<br>Catalysis B: Environmental, 2012, 125, 418-424.  | 20.2 | 174       |
| 26 | Enhanced Fenton-like degradation of pharmaceuticals over framework copper species in copper-doped mesoporous silica microspheres. Chemical Engineering Journal, 2015, 274, 298-306.  | 12.7 | 170       |
| 27 | Enhanced fluoride adsorption using Al (III) modified calcium hydroxyapatite. Journal of Hazardous<br>Materials, 2012, 233-234, 194-199.  | 12.4 | 167       |
| 28 | Transformation of humic acid and halogenated byproduct formation in UV-chlorine processes. Water Research, 2016, 102, 421-427.   | 11.3 | 164       |
| 29 | Photocatalytic degradation of triazine-containing azo dyes in aqueous TiO2 suspensions. Applied<br>Catalysis B: Environmental, 2003, 42, 47-55.  | 20.2 | 159       |
| 30 | Efficient Fenton-like Process for Pollutant Removal in Electron-Rich/Poor Reaction Sites Induced by<br>Surface Oxygen Vacancy over Cobalt–Zinc Oxides. Environmental Science & Technology, 2020, 54,<br>8333-8343.                                     | 10.0 | 137       |
| 31 | Selective H <sub>2</sub> O <sub>2</sub> conversion to hydroxyl radicals in the electron-rich area of<br>hydroxylated C-g-C <sub>3</sub> N <sub>4</sub> /CuCo–Al <sub>2</sub> O <sub>3</sub> . Journal of<br>Materials Chemistry A, 2017, 5, 7153-7164. | 10.3 | 136       |
| 32 | Catalytic ozonation of toxic pollutants over magnetic cobalt and manganese co-doped Î <sup>3</sup> -Fe2O3. Applied<br>Catalysis B: Environmental, 2010, 100, 62-67.  | 20.2 | 131       |
| 33 | Enhanced degradation of organic pollutants over Cu-doped LaAlO3 perovskite through<br>heterogeneous Fenton-like reactions. Chemical Engineering Journal, 2018, 332, 572-581.   | 12.7 | 131       |
| 34 | Preparation and visible-light photocatalytic activity of Ag3VO4 powders. Journal of Solid State Chemistry, 2007, 180, 725-732.   | 2.9  | 122       |
| 35 | Catalytic ozonation of toxic pollutants over magnetic cobalt-doped Fe3O4 suspensions. Applied<br>Catalysis B: Environmental, 2012, 117-118, 246-252.   | 20.2 | 120       |
| 36 | Photoelectrocatalytic Degradation of Triazine-Containing Azo Dyes at<br>γ-Bi <sub>2</sub> MoO <sub>6</sub> Film Electrode under Visible Light Irradiation (λ > 420 Nm).<br>Environmental Science & Technology, 2007, 41, 6802-6807.                    | 10.0 | 118       |

| #  | Article   | IF   | CITATIONS |
|----|---|------|-----------|
| 37 | Characterization and Reactivity of MnO <sub><i>x</i></sub> Supported on Mesoporous Zirconia for<br>Herbicide 2,4-D Mineralization with Ozone. Environmental Science & Technology, 2008, 42,<br>3363-3368. | 10.0 | 118       |
| 38 | Surface acidity and reactivity of β-FeOOH/Al2O3 for pharmaceuticals degradation with ozone: In situ ATR-FTIR studies. Applied Catalysis B: Environmental, 2010, 97, 340-346.                              | 20.2 | 118       |
| 39 | Enhanced catalytic degradation of ciprofloxacin over Ce-doped OMS-2 microspheres. Applied Catalysis<br>B: Environmental, 2016, 181, 561-569.  | 20.2 | 118       |
| 40 | Decolorization of methylene blue in layered manganese oxide suspension with H2O2. Journal of<br>Hazardous Materials, 2011, 190, 780-785.  | 12.4 | 109       |
| 41 | Enhanced Fenton-like degradation of refractory organic compounds by surface complex formation of LaFeO3 and H2O2. Journal of Hazardous Materials, 2015, 294, 195-200.                                     | 12.4 | 107       |
| 42 | Enhanced mineralization of pharmaceuticals by surface oxidation over mesoporous Î <sup>3</sup> -Ti-Al2O3 suspension with ozone. Applied Catalysis B: Environmental, 2017, 202, 118-126.                   | 20.2 | 107       |
| 43 | Highly nitrogen-doped porous carbon transformed from graphitic carbon nitride for efficient metal-free catalysis. Journal of Hazardous Materials, 2020, 393, 121280.                                      | 12.4 | 105       |
| 44 | Self-assembled synthesis of benzene-ring-grafted g-C3N4 nanotubes for enhanced photocatalytic H2 evolution. Applied Catalysis B: Environmental, 2020, 279, 119401.  | 20.2 | 104       |
| 45 | Photocatalytic degradation of cationic blue X-GRL adsorbed on TiO2/SiO2 photocatalyst. Applied Catalysis B: Environmental, 2003, 40, 131-140.   | 20.2 | 103       |
| 46 | Characterization of biofilm and corrosion of cast iron pipes in drinking water distribution system with UV/Cl2 disinfection. Water Research, 2014, 60, 174-181.   | 11.3 | 101       |
| 47 | p-AgI anchored on {001} facets of n-Bi2O2CO3 sheets with enhanced photocatalytic activity and stability. Applied Catalysis B: Environmental, 2017, 205, 34-41.  | 20.2 | 97        |
| 48 | Coordination Number Dependent Catalytic Activity of Singleâ€Atom Cobalt Catalysts for Fentonâ€Like<br>Reaction. Advanced Functional Materials, 2022, 32, .  | 14.9 | 87        |
| 49 | Efficient destruction of pathogenic bacteria with AgBr/TiO2 under visible light irradiation. Applied<br>Catalysis B: Environmental, 2007, 73, 354-360.  | 20.2 | 86        |
| 50 | Framework Cu-doped AlPO4 as an effective Fenton-like catalyst for bisphenol A degradation. Applied<br>Catalysis B: Environmental, 2017, 207, 9-16.  | 20.2 | 86        |
| 51 | Photoassisted degradation of endocrine disruptors over CuOx–FeOOH with H2O2 at neutral pH.<br>Applied Catalysis B: Environmental, 2009, 87, 30-36.  | 20.2 | 84        |
| 52 | Efficient Destruction of Pathogenic Bacteria with NiO/SrBi2O4under Visible Light Irradiation.<br>Environmental Science & Technology, 2006, 40, 5508-5513.   | 10.0 | 81        |
| 53 | Nanoporous Silica-Supported Nanometric Palladium:Â Synthesis, Characterization, and Catalytic Deep<br>Oxidation of Benzene. Environmental Science & Technology, 2005, 39, 1319-1323.                      | 10.0 | 80        |
| 54 | Construction of g-C3N4/WO3/MoS2 ternary nanocomposite with enhanced charge separation and collection for efficient wastewater treatment under visible light. Chemosphere, 2020, 247, 125784.              | 8.2  | 80        |

| #  | Article  | IF   | CITATIONS |
|----|--|------|-----------|
| 55 | Efficient inhibition of photogenerated electron-hole recombination through persulfate activation<br>and dual-pathway degradation of micropollutants over iron molybdate. Applied Catalysis B:<br>Environmental, 2019, 257, 117904.                                 | 20.2 | 79        |
| 56 | Synergistic effect of the sequential use of UV irradiation and chlorine to disinfect reclaimed water.<br>Water Research, 2012, 46, 1225-1232.  | 11.3 | 77        |
| 57 | Origin of the Excellent Activity and Selectivity of a Single-Atom Copper Catalyst with Unsaturated<br>Cu-N <sub>2</sub> Sites via Peroxydisulfate Activation: Cu(III) as a Dominant Oxidizing Species.<br>Environmental Science & Technology, 2022, 56, 8765-8775. | 10.0 | 77        |
| 58 | Zn:ln(OH) <sub><i>y</i></sub> S <sub><i>z</i></sub> Solid Solution Nanoplates: Synthesis,<br>Characterization, and Photocatalytic Mechanism. Environmental Science & Technology, 2009, 43,<br>7883-7888.   | 10.0 | 76        |
| 59 | Plasmon-Induced Inactivation of Enteric Pathogenic Microorganisms with<br>Agâ^'AgI/Al <sub>2</sub> O <sub>3</sub> under Visible-Light Irradiation. Environmental Science &<br>Technology, 2010, 44, 7058-7062.   | 10.0 | 76        |
| 60 | Photoproducts of tetracycline and oxytetracycline involving self-sensitized oxidation in aqueous solutions: Effects of Ca2+ and Mg2+. Journal of Environmental Sciences, 2011, 23, 1634-1639.  | 6.1  | 75        |
| 61 | Enhanced internal electric field in S-doped BiOBr for intercalation, adsorption and degradation of ciprofloxacin by photoinitiation. Applied Catalysis B: Environmental, 2022, 302, 120824.  | 20.2 | 75        |
| 62 | Internal electric field construction on dual oxygen group-doped carbon nitride for enhanced<br>photodegradation of pollutants under visible light irradiation. Applied Catalysis B: Environmental,<br>2019, 256, 117705.   | 20.2 | 74        |
| 63 | Enhanced Fenton-catalytic efficiency by highly accessible active sites on dandelion-like<br>copper–aluminum–silica nanospheres for water purification. Journal of Materials Chemistry A, 2016,<br>4, 8610-8619.  | 10.3 | 73        |
| 64 | A dual-reaction-center Fenton-like process on –Cî€,N–Cu linkage between copper oxides and<br>defect-containing g-C <sub>3</sub> N <sub>4</sub> for efficient removal of organic pollutants.<br>Journal of Materials Chemistry A, 2018, 6, 17819-17828.             | 10.3 | 73        |
| 65 | Characterization and photocatalytic activity of noble-metal-supported surface TiO2/SiO2. Applied<br>Catalysis A: General, 2003, 253, 389-396.  | 4.3  | 72        |
| 66 | Two-dimensional graphene/g-C3N4 in-plane hybrid heterostructure for enhanced photocatalytic<br>activity with surface-adsorbed pollutants assistant. Applied Catalysis B: Environmental, 2020, 268,<br>118397.  | 20.2 | 71        |
| 67 | General synthesis of carbon and oxygen dual-doped graphitic carbon nitride via copolymerization for non-photochemical oxidation of organic pollutant. Journal of Hazardous Materials, 2020, 394, 122578.   | 12.4 | 71        |
| 68 | Cationâ^'ï€ structure inducing efficient peroxymonosulfate activation for pollutant degradation over<br>atomically dispersed cobalt bonding graphene-like nanospheres. Applied Catalysis B: Environmental,<br>2021, 286, 119912.                                   | 20.2 | 71        |
| 69 | Catalytic Ozonation of Herbicide 2,4-D over Cobalt Oxide Supported on Mesoporous Zirconia. Journal of Physical Chemistry C, 2008, 112, 5978-5983.  | 3.1  | 70        |
| 70 | Galvanic-like cells produced by negative charge nonuniformity of lattice oxygen on<br>d-TiCuAl–SiO <sub>2</sub> nanospheres for enhancement of Fenton-catalytic efficiency.<br>Environmental Science: Nano, 2016, 3, 1483-1492.                                    | 4.3  | 68        |
| 71 | Facile synthesis of nitrogen-deficient mesoporous graphitic carbon nitride for highly efficient photocatalytic performance. Applied Surface Science, 2019, 478, 304-312.   | 6.1  | 68        |
| 72 | Characteristics of biofilms and iron corrosion scales with ground and surface waters in drinking water distribution systems. Corrosion Science, 2015, 90, 331-339.   | 6.6  | 67        |

| #  | Article  | IF   | CITATIONS |
|----|--|------|-----------|
| 73 | Efficient destruction of bacteria with Ti(IV) and antibacterial ions in co-substituted hydroxyapatite<br>films. Applied Catalysis B: Environmental, 2007, 73, 345-353.   | 20.2 | 65        |
| 74 | Enhanced photoactivity of Bi2WO6 by iodide insertion into the interlayer for water purification under visible light. Chemical Engineering Journal, 2018, 352, 664-672.   | 12.7 | 65        |
| 75 | Preparation and visible-light activity of silver vanadate for the degradation of pollutants. Materials<br>Research Bulletin, 2008, 43, 2986-2997.  | 5.2  | 64        |
| 76 | Inhibition of bromate formation by surface reduction in catalytic ozonation of organic pollutants over β-FeOOH/Al2O3. Applied Catalysis B: Environmental, 2014, 147, 287-292.  | 20.2 | 64        |
| 77 | Fe-N-Graphene Wrapped Al <sub>2</sub> O <sub>3</sub> /Pentlandite from Microalgae: High Fenton<br>Catalytic Efficiency from Enhanced Fe <sup>3+</sup> Reduction. Environmental Science &<br>Technology, 2018, 52, 3608-3614. | 10.0 | 64        |
| 78 | Effect of sequential UV/free chlorine disinfection on opportunistic pathogens and microbial community structure in simulated drinking water distribution systems. Chemosphere, 2019, 219, 971-980.                           | 8.2  | 64        |
| 79 | Insights into the difference in metal-free activation of peroxymonosulfate and peroxydisulfate.<br>Chemical Engineering Journal, 2020, 394, 123936.  | 12.7 | 63        |
| 80 | Influence of pretreatment conditions on low-temperature CO oxidation over Au/MOx/Al2O3 catalysts.<br>Journal of Molecular Catalysis A, 2003, 200, 229-238.   | 4.8  | 62        |
| 81 | Porous β-Bi2O3 with multiple vacancy associates on highly exposed active {220} facets for enhanced photocatalytic activity. Applied Catalysis B: Environmental, 2020, 265, 118563.   | 20.2 | 62        |
| 82 | Effects of microbial redox cycling of iron on cast iron pipe corrosion in drinking water distribution systems. Water Research, 2014, 65, 362-370.  | 11.3 | 61        |
| 83 | Enhanced polarization of electron-poor/rich micro-centers over nZVCu-Cu(II)-rGO for pollutant removal with H2O2. Journal of Hazardous Materials, 2020, 383, 121182.  | 12.4 | 61        |
| 84 | Characterization and reactivity of biogenic manganese oxides for ciprofloxacin oxidation. Journal of<br>Environmental Sciences, 2014, 26, 1154-1161.   | 6.1  | 60        |
| 85 | Enhanced photocatalytic performance by the synergy of Bi vacancies and BiO in BiO-Bi2-ÎMoO6. Applied<br>Catalysis B: Environmental, 2019, 257, 117785.   | 20.2 | 60        |
| 86 | Efficient Fenton-like Process Induced by Fortified Electron-Rich O Microcenter on the Reduction State<br>Cu-Doped CNO Polymer. ACS Applied Materials & Interfaces, 2019, 11, 16496-16505.                                    | 8.0  | 59        |
| 87 | Effects of phosphate-enhanced ozone/biofiltration on formation of disinfection byproducts and occurrence of opportunistic pathogens in drinking water distribution systems. Water Research, 2018, 139, 168-176.              | 11.3 | 58        |
| 88 | Catalytic combustion of methane on novel catalysts derived from Cu-Mg/Al-hydrotalcites. Catalysis<br>Letters, 2005, 99, 157-163.   | 2.6  | 55        |
| 89 | Photocatalytic decomposition of acetaldehyde and Escherichia coli using NiO/SrBi2O4 under visible<br>light irradiation. Applied Catalysis B: Environmental, 2006, 69, 17-23.   | 20.2 | 55        |
| 90 | Efficient photodegradation of Acid Red B by immobilized ferrocene in the presence of UVA and H2O2.<br>Journal of Hazardous Materials, 2008, 154, 146-152.  | 12.4 | 55        |

| #   | Article  | IF   | CITATIONS |
|-----|--|------|-----------|
| 91  | Enhanced Cr(VI) reduction by direct transfer of photo-generated electrons to Cr 3d orbitals in<br>CrO42intercalated BiOBr with exposed (110) facets. Applied Catalysis B: Environmental, 2020, 277,<br>119065.   | 20.2 | 55        |
| 92  | Framework Cu-doped boron nitride nanobelts with enhanced internal electric field for effective<br>Fenton-like removal of organic pollutants. Journal of Materials Chemistry A, 2019, 7, 6946-6956.   | 10.3 | 54        |
| 93  | Engineering the low-coordinated single cobalt atom to boost persulfate activation for enhanced organic pollutant oxidation. Applied Catalysis B: Environmental, 2022, 303, 120877.   | 20.2 | 54        |
| 94  | Simple Amphoteric Charge Strategy to Reinforce Superhydrophilic Polyvinylidene Fluoride Membrane<br>for Highly Efficient Separation of Various Surfactant-Stabilized Oil-in-Water Emulsions. ACS Applied<br>Materials & Interfaces, 2020, 12, 47018-47028. | 8.0  | 52        |
| 95  | Photolysis of Chlortetracycline in aqueous solution: Kinetics, toxicity and products. Journal of<br>Environmental Sciences, 2012, 24, 254-260.   | 6.1  | 51        |
| 96  | AgBr-wrapped Ag chelated on nitrogen-doped reduced graphene oxide for water purification under visible light. Applied Catalysis B: Environmental, 2018, 220, 118-125.  | 20.2 | 51        |
| 97  | Degradation characteristics of humic acid over iron oxides/Fe0 core–shell nanoparticles with<br>UVA/H2O2. Journal of Hazardous Materials, 2010, 173, 474-479.  | 12.4 | 50        |
| 98  | Efficient Fenton-like process for organic pollutant degradation on Cu-doped mesoporous polyimide nanocomposites. Environmental Science: Nano, 2019, 6, 798-808.  | 4.3  | 49        |
| 99  | Hierarchically Active Poly(vinylidene fluoride) Membrane Fabricated by In Situ Generated Zero-Valent<br>Iron for Fouling Reduction. ACS Applied Materials & Interfaces, 2020, 12, 10993-11004.   | 8.0  | 49        |
| 100 | Response of microorganisms in biofilm to sulfadiazine and ciprofloxacin in drinking water distribution systems. Chemosphere, 2019, 218, 197-204.   | 8.2  | 48        |
| 101 | Nitrogen-Coordinated Cobalt Embedded in a Hollow Carbon Polyhedron for Superior Catalytic<br>Oxidation of Organic Contaminants with Peroxymonosulfate. ACS ES&T Engineering, 2021, 1, 76-85.   | 7.6  | 48        |
| 102 | Characterization and catalytic performance of Co/SBA-15 supported gold catalysts for CO oxidation.<br>Materials Research Bulletin, 2006, 41, 406-413.  | 5.2  | 47        |
| 103 | Photoassisted Degradation of Azodyes over FeOxH2x-3/FeO in the Presence of H2O2 at Neutral pH<br>Values. Environmental Science & Technology, 2007, 41, 4715-4719.  | 10.0 | 47        |
| 104 | In situ generation and efficient activation of H2O2 for pollutant degradation over CoMoS2<br>nanosphere-embedded rGO nanosheets and its interfacial reaction mechanism. Journal of Colloid and<br>Interface Science, 2019, 543, 214-224.                   | 9.4  | 47        |
| 105 | One-year survey of opportunistic premise plumbing pathogens and free-living amoebae in the tap-water of one northern city of China. Journal of Environmental Sciences, 2019, 77, 20-31.  | 6.1  | 46        |
| 106 | Sustaining reactivity of FeO for nitrate reduction via electron transfer between dissolved Fe2+ and surface iron oxides. Journal of Hazardous Materials, 2016, 308, 208-215.   | 12.4 | 45        |
| 107 | Enhanced azo dye decolorization through charge transmission by σ-Sb3+-azo complexes on amorphous<br>Sb2S3 under visible light irradiation. Applied Catalysis B: Environmental, 2019, 240, 132-140.   | 20.2 | 45        |
| 108 | Theoretical and experimental evidence for rGO-4-PP Nc as a metal-free Fenton-like catalyst by tuning the electron distribution. RSC Advances, 2018, 8, 3312-3320.  | 3.6  | 44        |

| #   | Article  | IF   | CITATIONS |
|-----|--|------|-----------|
| 109 | Sulfadiazine/ciprofloxacin promote opportunistic pathogens occurrence in bulk water of drinking water distribution systems. Environmental Pollution, 2018, 234, 71-78.   | 7.5  | 42        |
| 110 | Characterization of the bacterial communities and iron corrosion scales in drinking groundwater distribution systems with chlorine/chloramine. International Biodeterioration and Biodegradation, 2014, 96, 71-79.   | 3.9  | 41        |
| 111 | Characterization and adsorption performance of Zrâ€doped akaganéite for efficient arsenic removal.<br>Journal of Chemical Technology and Biotechnology, 2013, 88, 629-635.   | 3.2  | 40        |
| 112 | Oxygen vacancy enhanced photostability and activity of plasmon-Ag composites in the visible to near-infrared region for water purification. Applied Catalysis B: Environmental, 2016, 199, 230-240.  | 20.2 | 40        |
| 113 | Photoelectrochemical degradation of Methylene Blue with β-PbO2 electrodes driven by visible light<br>irradiation. Journal of Environmental Sciences, 2011, 23, 998-1003.   | 6.1  | 39        |
| 114 | Enhanced solar photodegradation of toxic pollutants by long-lived electrons in Ag–Ag2O nanocomposites. Applied Catalysis B: Environmental, 2015, 176-177, 637-645.   | 20.2 | 38        |
| 115 | Efficient solar hydrogen production coupled with organics degradation by a hybrid tandem<br>photocatalytic fuel cell using a silicon-doped TiO2 nanorod array with enhanced electronic<br>properties. Journal of Hazardous Materials, 2020, 394, 121425.     | 12.4 | 38        |
| 116 | Efficient removal of disinfection by-products precursors and inhibition of bacterial detachment by strong interaction of EPS with coconut shell activated carbon in ozone/biofiltration. Journal of Hazardous Materials, 2020, 392, 122077.                  | 12.4 | 38        |
| 117 | The abatement of major pollutants in air and water by environmental catalysis. Frontiers of Environmental Science and Engineering, 2013, 7, 302-325.   | 6.0  | 37        |
| 118 | A self-sustaining monolithic photoelectrocatalytic/photovoltaic system based on a WO3/BiVO4<br>photoanode and Si PVC for efficiently producing clean energy from refractory organics degradation.<br>Applied Catalysis B: Environmental, 2018, 238, 309-317. | 20.2 | 37        |
| 119 | Enhanced inhibition of bromate formation in catalytic ozonation of organic pollutants over Fe–Al LDH/Al2O3. Separation and Purification Technology, 2015, 151, 256-261.  | 7.9  | 36        |
| 120 | Dual-reaction-center catalytic process continues Fenton's story. Frontiers of Environmental Science<br>and Engineering, 2020, 14, 1.   | 6.0  | 36        |
| 121 | Notable light-free catalytic activity for pollutant destruction over flower-like BiOI microspheres by a dual-reaction-center Fenton-like process. Journal of Colloid and Interface Science, 2018, 527, 251-259.  | 9.4  | 35        |
| 122 | Exfoliated and plicated g-C3N4 nanosheets for efficient photocatalytic organic degradation and hydrogen evolution. International Journal of Hydrogen Energy, 2021, 46, 20547-20559.  | 7.1  | 34        |
| 123 | Removal of persistent organic pollutants from micro-polluted drinking water by triolein embedded absorbent. Bioresource Technology, 2009, 100, 2995-3002.  | 9.6  | 33        |
| 124 | Treatment of NOM fractions of reservoir sediments: Effect of UV and chlorination on formation of DBPs. Separation and Purification Technology, 2015, 154, 228-235.   | 7.9  | 32        |
| 125 | Impacts of bacteria and corrosion on removal of natural organic matter and disinfection byproducts in different drinking water distribution systems. International Biodeterioration and Biodegradation, 2017, 117, 52-59.                                    | 3.9  | 32        |
| 126 | An efficient electron transfer at the Fe0/iron oxide interface for the photoassisted degradation of pollutants with H2O2. Applied Catalysis B: Environmental, 2008, 82, 151-156.   | 20.2 | 31        |

| #   | Article   | lF         | CITATIONS          |
|-----|---|------------|--------------------|
| 127 | <scp>l</scp> -Ascorbic acid oxygen-induced micro-electronic fields over metal-free polyimide for<br>peroxymonosulfate activation to realize efficient multi-pathway destruction of contaminants.<br>Journal of Materials Chemistry A, 2020, 8, 810-819.   | 10.3       | 31                 |
| 128 | Enhanced Fenton-like efficiency by the synergistic effect of oxygen vacancies and organics adsorption on FexOy-d-g-C3N4 with Fe‒N complexation. Journal of Hazardous Materials, 2021, 408, 124818.  | 12.4       | 31                 |
| 129 | Sequential use of ultraviolet light and chlorine for reclaimed water disinfection. Journal of Environmental Sciences, 2011, 23, 1605-1610.  | 6.1        | 30                 |
| 130 | Characteristics of corrosion sales and biofilm in aged pipe distribution systems with switching water source. Engineering Failure Analysis, 2016, 60, 166-175.  | 4.0        | 29                 |
| 131 | Cu-doped Bi2O3/Bi0 composite as an efficient Fenton-like catalyst for degradation of 2-chlorophenol.<br>Separation and Purification Technology, 2016, 157, 203-208.   | 7.9        | 29                 |
| 132 | Interaction of ciprofloxacin chlorination products with bacteria in drinking water distribution systems. Journal of Hazardous Materials, 2017, 339, 174-181.  | 12.4       | 29                 |
| 133 | Effects of combined UV and chlorine disinfection on corrosion and water quality within reclaimed water distribution systems. Engineering Failure Analysis, 2014, 39, 12-20.   | 4.0        | 27                 |
| 134 | Characterization and photostability of Cu2O–Ag–AgBr/Al2O3 for the degradation of toxic pollutants<br>with visible-light irradiation. Applied Catalysis B: Environmental, 2014, 154-155, 44-50.  | 20.2       | 27                 |
| 135 | Effects of microbial cycling of Fe(II)/Fe(III) and Fe/N on cast iron corrosion in simulated drinking water distribution systems. Corrosion Science, 2015, 100, 599-606.   | 6.6        | 27                 |
| 136 | Chemical-bond conjugated BiO(OH)xI1-x-AgI heterojunction with high visible light activity and stability in degradation of pollutants. Applied Catalysis B: Environmental, 2017, 218, 443-451.   | 20.2       | 27                 |
| 137 | Effects of O3/Cl2 disinfection on corrosion and opportunistic pathogens growth in drinking water distribution systems. Journal of Environmental Sciences, 2018, 73, 38-46.  | 6.1        | 27                 |
| 138 | Highly improved photoelectrocatalytic efficiency and stability of WO <sub>3</sub> photoanodes by<br>the facile <i>in situ</i> growth of TiO <sub>2</sub> branch overlayers. Nanoscale, 2018, 10, 13393-13401.   | 5.6        | 27                 |
| 139 | Enhancing photocatalytic performance by direct photo-excited electron transfer from organic<br>pollutants to low-polymerized graphitic carbon nitride with more C-NH/NH2 exposure. Applied<br>Catalysis B: Environmental, 2021, 296, 120316.  | 20.2       | 26                 |
| 140 | Effects of inorganic anions on photoactivity of various photocatalysts under different conditions.<br>Journal of Chemical Technology and Biotechnology, 2004, 79, 247-252.  | 3.2        | 25                 |
| 141 | Inhibition mechanism of <mml:math xmlns:mml="http://www.w3.org/1998/Math/Math/ML&lt;br">altimg="sil.gif"<br/>overflow="scroll"&gt;<mml:mrow> <mml:msubsup> <mml:mrow> <mml:mtext>BrO</mml:mtext> </mml:mrow> <mml<br>formation over MnO /Al2O3 during the catalytic ozonation of 2,4-dichlorophenoxyacetic acid in</mml<br></mml:msubsup></mml:mrow></mml:math> | :m///ww><1 | mı <b>2ıå</b> mn>3 |
| 142 | water. Separation and Purfication Technology, 2013, 117, 41945.<br>Efficient catalytic aerobic oxidation ofÂchlorinated phenols with mixed-valent manganese oxide<br>nanoparticles. Journal of Chemical Technology and Biotechnology, 2015, 90, 80-86.  | 3.2        | 25                 |
| 143 | Ï€-Ï€ conjugation driving degradation of aromatic compounds with in-situ hydrogen peroxide<br>generation over Zn2ln2S5 grown on nitrogen-doped carbon spheres. Applied Catalysis B:<br>Environmental, 2022, 310, 121298.  | 20.2       | 25                 |
| 144 | Carbonized MOF-Coated Zero-Valent Cu Driving an Efficient Dual-Reaction-Center Fenton-like Water<br>Treatment Process through Utilizing Pollutants and Natural Dissolved Oxygen. ACS ES&T Water, 2022,<br>2, 174-183.   | 4.6        | 25                 |

| #   | Article  | IF   | CITATIONS |
|-----|--|------|-----------|
| 145 | Effects of NOM on the degradation of chloramphenicol by UV/H2O2 and the characteristics of degradation products. Separation and Purification Technology, 2018, 191, 108-115.   | 7.9  | 24        |
| 146 | Efficient light-free activation of peroxymonosulfate by carbon ring conjugated carbon nitride for elimination of organic pollutants. Chemical Engineering Journal, 2021, 420, 129671.  | 12.7 | 24        |
| 147 | Detoxification and selective separation of Cr(VI) and As(III) in wastewater based on interfacial coupling in BiOBr with {110} facet under visible-light irradiation. Applied Catalysis B: Environmental, 2022, 307, 121192.                      | 20.2 | 24        |
| 148 | Enhanced photocatalytic destruction of pollutants by surface W vacancies in VW-Bi2WO6 under visible light. Journal of Colloid and Interface Science, 2020, 576, 385-393.   | 9.4  | 23        |
| 149 | More octahedral Cu+ and surface acid sites in uniformly porous Cu-Al2O3 for enhanced Fenton catalytic performances. Journal of Hazardous Materials, 2021, 406, 124739.   | 12.4 | 23        |
| 150 | Characterization of biofilm bacterial communities and cast iron corrosion in bench-scale reactors with chloraminated drinking water. Engineering Failure Analysis, 2015, 57, 423-433.  | 4.0  | 22        |
| 151 | Mesoporous reduction state cobalt species-doped silica nanospheres: An efficient Fenton-like catalyst<br>for dual-pathway degradation of organic pollutants. Journal of Colloid and Interface Science, 2020,<br>576, 59-67.                      | 9.4  | 22        |
| 152 | H2O2 inducing dissolved oxygen activation and electron donation of pollutants over Fe-ZnS quantum<br>dots through surface electron-poor/rich microregion construction for water treatment. Journal of<br>Hazardous Materials, 2021, 420, 126579. | 12.4 | 22        |
| 153 | Enhanced photocatalytic efficiency by direct photoexcited electron transfer from pollutants<br>adsorbed on the surface valence band of BiOBr modified with graphitized C. Journal of Hazardous<br>Materials, 2022, 424, 127502.                  | 12.4 | 22        |
| 154 | Effects of disinfection efficiency on microbial communities and corrosion processes in drinking water distribution systems simulated with actual running conditions. Journal of Environmental Sciences, 2020, 88, 273-282.                       | 6.1  | 21        |
| 155 | Phototransformation of nitrobenzene in the Songhua River: Kinetics and photoproduct analysis.<br>Journal of Environmental Sciences, 2008, 20, 787-795.   | 6.1  | 20        |
| 156 | One-step scalable synthesis of honeycomb-like g-C <sub>3</sub> N <sub>4</sub> with broad sub-bandgap<br>absorption for superior visible-light-driven photocatalytic hydrogen evolution. RSC Advances, 2019, 9,<br>32674-32682.                   | 3.6  | 20        |
| 157 | Highly Efficient Hydrogen and Electricity Production Combined with Degradation of Organics Based<br>on a Novel Solar Water-Energy Nexus System. ACS Applied Materials & Interfaces, 2020, 12,<br>2505-2515.                                      | 8.0  | 20        |
| 158 | Heterogeneous Fenton-like reaction followed by GAC filtration improved removal efficiency of NOM and DBPs without adjusting pH. Separation and Purification Technology, 2021, 260, 118234.   | 7.9  | 20        |
| 159 | Cation-Ï€ induced surface cleavage of organic pollutants with â‹OH formation from H2O for water treatment. IScience, 2021, 24, 102874.   | 4.1  | 20        |
| 160 | Adsorption and removal of arsenite on ordered mesoporous Fe-modified ZrO <sub>2</sub> .<br>Desalination and Water Treatment, 2009, 8, 139-145.   | 1.0  | 19        |
| 161 | O3-BAC-Cl2: A multi-barrier process controlling the regrowth of opportunistic waterborne<br>pathogens in drinking water distribution systems. Journal of Environmental Sciences, 2019, 76, 142-153.  | 6.1  | 19        |
| 162 | Surface sulfur vacancies enhanced electron transfer over Co-ZnS quantum dots for efficient<br>degradation of plasticizer micropollutants by peroxymonosulfate activation. Chinese Chemical<br>Letters, 2022, 33, 3829-3834.                      | 9.0  | 19        |

| #   | Article   | IF   | CITATIONS |
|-----|---|------|-----------|
| 163 | Nanoconfinement-Regulated Peroxymonosulfate Activation via an Anomalously Efficient Mediated Electron-Transfer Pathway on Cobalt. ACS ES&T Engineering, 2022, 2, 2014-2022.   | 7.6  | 19        |
| 164 | Preparation and evaluation of Zr-β-FeOOH for efficient arsenic removal. Journal of Environmental Sciences, 2013, 25, 815-822.   | 6.1  | 18        |
| 165 | Efficient Decomposition of Organic Pollutants over<br>nZVI/FeO <sub><i>x</i></sub> /FeN <sub><i>y</i></sub> -Anchored NC Layers via a Novel<br>Dual-Reaction-Centers-Based Wet Air Oxidation Process under Natural Conditions. ACS ES&T<br>Engineering, 2021, 1, 1333-1341. | 7.6  | 17        |
| 166 | The control of red water occurrence and opportunistic pathogens risks in drinking water distribution systems: A review. Journal of Environmental Sciences, 2021, 110, 92-98.  | 6.1  | 17        |
| 167 | Tailoring aromatic ring-terminated edges of g-C <sub>3</sub> N <sub>4</sub> nanosheets for efficient photocatalytic hydrogen evolution with simultaneous antibiotic removal. Catalysis Science and Technology, 2020, 10, 5470-5479.   | 4.1  | 16        |
| 168 | Enhanced Fenton-like process via interfacial electron donating of pollutants over in situ<br>Cobalt-doped graphitic carbon nitride. Journal of Colloid and Interface Science, 2022, 608, 673-682.   | 9.4  | 16        |
| 169 | Synthesis of MCM-48 with a high thermal and hydro-thermal stability. Materials Research Bulletin, 2005, 40, 1775-1780.  | 5.2  | 15        |
| 170 | Preparation of grape-like Bi2O3/Ti photoanode and its visible light activity. Materials Research<br>Bulletin, 2011, 46, 153-157.  | 5.2  | 15        |
| 171 | Characterization of chemical composition and bacterial community of corrosion scales in different drinking water distribution systems. Environmental Science: Water Research and Technology, 2017, 3, 147-155.  | 2.4  | 15        |
| 172 | Enhanced Fenton-like catalytic performance of Cu-Al/KIT-6 and the key role of O2 in triggering reaction. Chemical Engineering Journal, 2020, 387, 124006.   | 12.7 | 15        |
| 173 | Vanadium tetrasulfide cross-linking graphene-like carbon driving a sustainable electron supply chain<br>from pollutants through the activation of dissolved oxygen and hydrogen peroxide. Environmental<br>Science: Nano, 2021, 8, 86-96.                                   | 4.3  | 15        |
| 174 | Enhanced Photodegradation of Toxic Pollutants on Plasmonic Au–Ag–AgI/Al2O3 Under Visible<br>Irradiation. Catalysis Letters, 2012, 142, 646-654.   | 2.6  | 14        |
| 175 | Enhanced electron transfer and silver-releasing suppression in Ag–AgBr/titanium-doped Al2O3<br>suspensions with visible-light irradiation. Journal of Hazardous Materials, 2012, 219-220, 276-282.  | 12.4 | 14        |
| 176 | Inhibiting the increase of antibiotic resistance genes during drinking water distribution by superior<br>microbial interface using Fe modified granular activated carbon. Journal of Cleaner Production, 2022,<br>335, 130225.  | 9.3  | 14        |
| 177 | Ï€-Ï€ conjugation driving peroxymonosulfate activation for pollutant elimination over metal-free<br>graphitized polyimide surface. Journal of Hazardous Materials, 2021, 412, 125191.   | 12.4 | 13        |
| 178 | Inactivation and Photorepair of Enteric Pathogenic Microorganisms with Ultraviolet Irradiation.<br>Environmental Engineering Science, 2012, 29, 549-553.  | 1.6  | 12        |
| 179 | Characterization of bacterial community and iron corrosion in drinking water distribution systems with O 3 -biological activated carbon treatment. Journal of Environmental Sciences, 2018, 69, 192-204.  | 6.1  | 12        |
| 180 | Enhanced •OH generation and pollutants removal by framework Cu doped LaAlO3/Al2O3. Journal of<br>Hazardous Materials, 2022, 431, 128578.  | 12.4 | 12        |

| #   | Article   | IF   | CITATIONS |
|-----|---|------|-----------|
| 181 | Efficient Removal of Toxic Pollutants Over Fe–Co/ZrO2 Bimetallic Catalyst with Ozone. Catalysis<br>Letters, 2012, 142, 1026-1032.   | 2.6  | 11        |
| 182 | Improving the charge properties of the WO <sub>3</sub> photoanode using a BiFeO <sub>3</sub> ferroelectric nanolayer. Physical Chemistry Chemical Physics, 2021, 23, 8241-8245.   | 2.8  | 11        |
| 183 | Few-layered Bi4O5I2 nanosheets enclosed by {1 0â^1} facets with oxygen vacancies for highly-efficient removal of water contaminants. Journal of Hazardous Materials, 2022, 437, 129274.   | 12.4 | 10        |
| 184 | Synthesize of Cu2O-CuO/Sr3BiO5.4 and its photocatalytic activity. Applied Surface Science, 2012, 258, 5955-5959.  | 6.1  | 9         |
| 185 | Catalytic ozonation performance and surface property of supported Fe3O4 catalysts dispersions.<br>Frontiers of Environmental Science and Engineering, 2013, 7, 451-456.   | 6.0  | 9         |
| 186 | The interaction of surface electron distribution-polarized Fe/polyimide hybrid nanosheets with organic pollutants driving a sustainable Fenton-like process. Materials Advances, 2020, 1, 1083-1091.  | 5.4  | 9         |
| 187 | Effects of cast iron pipe corrosion on nitrogenous disinfection by-products formation in drinking water distribution systems via interaction among iron particles, biofilms, and chlorine. Chemosphere, 2022, 292, 133364.                          | 8.2  | 9         |
| 188 | Rapid pollutant degradation by peroxymonosulfate <i>via</i> an unusual mediated-electron transfer pathway under spatial-confinement. RSC Advances, 2022, 12, 5236-5244.   | 3.6  | 9         |
| 189 | Graphitized Cu-β-cyclodextrin polymer driving an efficient dual-reaction-center Fenton-like process by<br>utilizing electrons of pollutants for water purification. Journal of Environmental Sciences, 2023, 126,<br>565-574.                       | 6.1  | 9         |
| 190 | Boosting the Extra Generation of Superoxide Radicals on Graphitic Carbon Nitride with Carbon<br>Vacancies by the Modification of Pollutant Adsorption for High-Performance Photocatalytic<br>Degradation. ACS ES&T Engineering, 2022, 2, 1296-1305. | 7.6  | 8         |
| 191 | Peroxymonosulfate as inducer driving interfacial electron donation of pollutants over oxygen-rich<br>carbon–nitrogen graphene-like nanosheets for water treatment. Journal of Colloid and Interface<br>Science, 2022, 622, 272-283.                 | 9.4  | 8         |
| 192 | The epoxidation of allyl alcohol on Ti-complex/MCM-48 catalyst. Microporous and Mesoporous Materials, 2008, 112, 133-137.   | 4.4  | 7         |
| 193 | Plasmonâ€induced reduction of bromate with Au–Ag–AgI/Al <sub>2</sub> O <sub>3</sub> under<br>visibleâ€light irradiation. Journal of Chemical Technology and Biotechnology, 2014, 89, 1425-1431.   | 3.2  | 7         |
| 194 | BiO(OH)x11-x solid solution with rich oxygen vacancies: interlayer guest hydroxyl for improved photocatalytic properties. Journal of Colloid and Interface Science, 2022, 605, 1-12.  | 9.4  | 7         |
| 195 | Sustainable micro-activation of dissolved oxygen driving pollutant conversion on Mo-enhanced zinc sulfide surface in natural conditions. Fundamental Research, 2023, 3, 422-429.  | 3.3  | 7         |
| 196 | Effects of chlorine and pipe material on biofilm development and structure in a reclaimed water distribution system. Water Science and Technology: Water Supply, 2012, 12, 362-371.   | 2.1  | 5         |
| 197 | Destruction of microbial stability in drinking water distribution systems by trace phosphorus polluted water source. Chemosphere, 2021, 275, 130032.  | 8.2  | 5         |
| 198 | Contribution of extracellular polymeric substances and microbial community on the safety of<br>drinking water quality: By mean of Cu/activated carbon biofiltration. Chemosphere, 2022, 286, 131686.  | 8.2  | 5         |

| #   | Article   | IF   | CITATIONS |
|-----|---|------|-----------|
| 199 | Ultrathin Bi <sub>4</sub> O <sub>5</sub> Br <sub>2</sub> nanosheets with surface oxygen vacancies<br>and strong interaction with Bi <sub>2</sub> O <sub>2</sub> CO <sub>3</sub> for highly efficient<br>removal of water contaminants. Environmental Science: Nano, 2022, 9, 1341-1352. | 4.3  | 5         |
| 200 | Enhancing inhibition of disinfection byproducts formation and opportunistic pathogens growth during drinking water distribution by Fe2O3/Coconut shell activated carbon. Environmental Pollution, 2021, 268, 115838.  | 7.5  | 4         |
| 201 | Efficient destruction of humic acid with a self-purification process in an Fe0-FeyCz/Fex-GZIF-8-rGO aqueous suspension. Chemical Engineering Journal, 2022, 446, 136625.  | 12.7 | 4         |
| 202 | Synthesis of Nanosize Mesoporous MCM-48 Material. Journal of Nanoscience and Nanotechnology, 2005, 5, 1752-1754.  | 0.9  | 3         |
| 203 | Selective photocatalytic degradation of azodyes in NiO/Ag <sub>3</sub> VO <sub>4</sub> suspension.<br>Journal of Chemical Technology and Biotechnology, 2010, 85, 1522-1527.  | 3.2  | 3         |
| 204 | Accelerated degradation of pollutants via a close interface connection in heterojunction, and special solid-liquid interactions. Journal of Colloid and Interface Science, 2019, 553, 598-605.  | 9.4  | 3         |
| 205 | Effect of Ammonia Thermal Treatment on the Structure and Activity of Titanium Oxide Photocatalysts.<br>Chinese Journal of Chemical Physics, 2006, 19, 355-361.  | 1.3  | 2         |
| 206 | Degradation of ofloxacin in aqueous solution with UV/H2O2. , 0, 72, 386-393.  |      | 2         |
| 207 | CoO anchored on boron nitride nanobelts for efficient removal of water contaminants by peroxymonosulfate activation. Chemical Engineering Journal, 2022, 430, 132915.   | 12.7 | 2         |
| 208 | Surface-Confined Destruction of Pollutants with H2O2 Assistance over Cu0@CuOx-N-Graphitic Carbon Suspensions. Journal of Physical Chemistry C, 2022, 126, 1366-1375.  | 3.1  | 2         |
| 209 | Solar Photocatalytic Disinfection by Nano-Ag-Based Photocatalyst. Green Chemistry and Sustainable Technology, 2017, , 129-153.  | 0.7  | 1         |